Supplementary Table 1: Data Collection and Processing Statistics

Data Set	**Native**	**Long axis**	**Short axis**
Space group	$P2_12_12_1$	$P2_12_12_1$	$P2_12_12_1$
a (Å)	43.55	43.61	43.33
b (Å)	81.19	81.02	81.27
c (Å)	181.66	181.54	175.70
Energy (keV)	8.04	12.800	12.660
Resolution (Å)	3.0	2.0	2.0
Total reflections	60220	315646	301709
Unique reflections	13085	44405	42969
Completeness (%)	96.3(94.3)	99.8 (99.6)	99.8(99.5)
I/ σ(I)	45.1 (30.2)	21.4 (11.7)	19.2 (10.1)
R_{sym} (%)	0.027 (0.045)	0.071 (0.203)	0.066 (0.173)

Experimental phase determination at 3.0 Å resolution

R_{Cullis}	Isomorphous (Long axis - native, Se-S):	0.841
	Anomalous (Long axis):	0.677
Phasing power	Isomorphous (Long axis - native, Se-S):	0.872
	Anomalous (Long axis):	1.48
Combined figure of merit before density modification acentric reflections:	0.554	
Figure of merit before density modification centric reflections:	0.356	

Refinement

Resolution (Å)	30.0-2.0	30.-2.0
Atoms (protein, GDP.ALF$_4^-$, Na^+, Mg^{2+}) (N)	5428	5330
Atoms (water)	613	315
Reflections F > 0 σ(F) (work set)	43506	42102
R factor (%)	18.6	19.8
R_{free} (%)	23.4	25.1
Average B factor (Å^2)	16.8	23.6
Rms ΔB bonded atoms (Å^2)	3.54	4.26
Rms bond lengths (Å)	0.011	0.009
Rms bond angles (°)	2.63	2.55

Values in parentheses refer to the highest resolution shell: 2.05-2.00 Å for "long axis" and "short axis" crystals, and 3.15-3.00 Å for the native data set.

R_{sym}= $\sum_h \sum_i \left| I_{h,i} - I_h \right| / \sum_h \sum_i I_{h,i}$

R_{Cullis} is the mean residual lack of closure error divided by either the observed rms isomorphous or anomalous differences.

The phasing power is the rms calculated ismorphous or anomalous differences divided by the rms lack of closure errors.

The figure of merit if the cosine of the expected phase error.

R factor= $\sum \left| F_{obs} - F_{calc} \right| / \sum F_{obs}$

R_{free} was calculated a 2% subset of all reflections that was not used in refinement.

Supplementary Table 2: Catalytic rate constants for basal and assembly-stimulated GTPase activities of wildtype dynamin and active site mutants

	Basal	Liposome-stimulated
Dynamin	**kcat (min^{-1})**	**kcat (min^{-1})**
WT	1.02 ± 0.14	230 ± 22.8
Q40A	0.60 ± 0.19	2.9 ± 0.94
Q40E	0.65 ± 0.06	7.92 ± 01.52
S41A	0.60 ± 0.07	73.4 ± 6.80
S41G	0.72 ± 0.10	78.6 ± 11.88
D180A	10.67 ± 0.41	19.3 ± 2.02
D180N	10.62 ± 1.00	42.6 ± 5.90

These data represent the average of at least three independent experiments with multiple independently purified batches of protein.

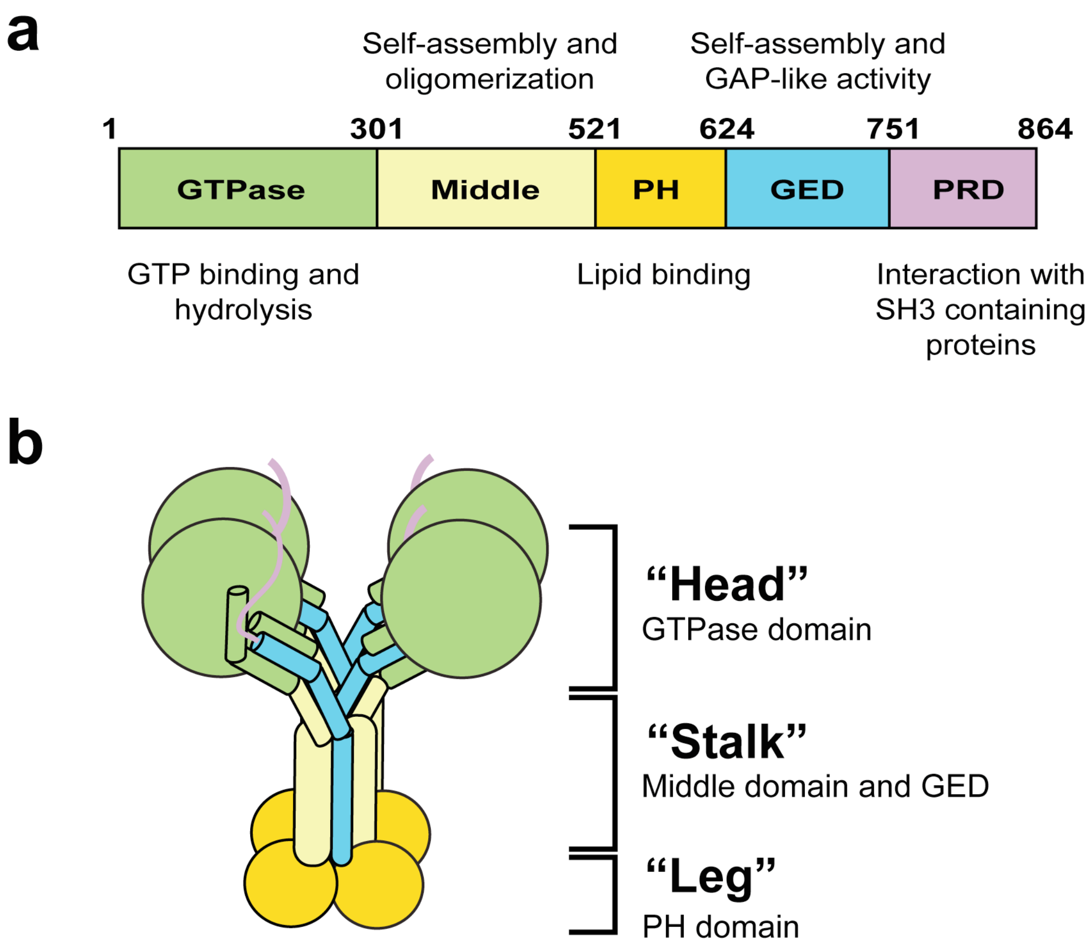

Supplementary Figure 1. Domain organization and quaternary structure of dynamin. a, Dynamin is a 96kD GTPase with five functionally distinct domains. b, Dynamin is a tetramer in solution. Cryo-electron microscopic reconstructions of dynamin assemblies on liposomes have suggested a domain organization in which the GTPase domain "heads" are supported by a "stalk" composed of the middle domain and GED, which connects to the membrane-bound PH domain "leg".

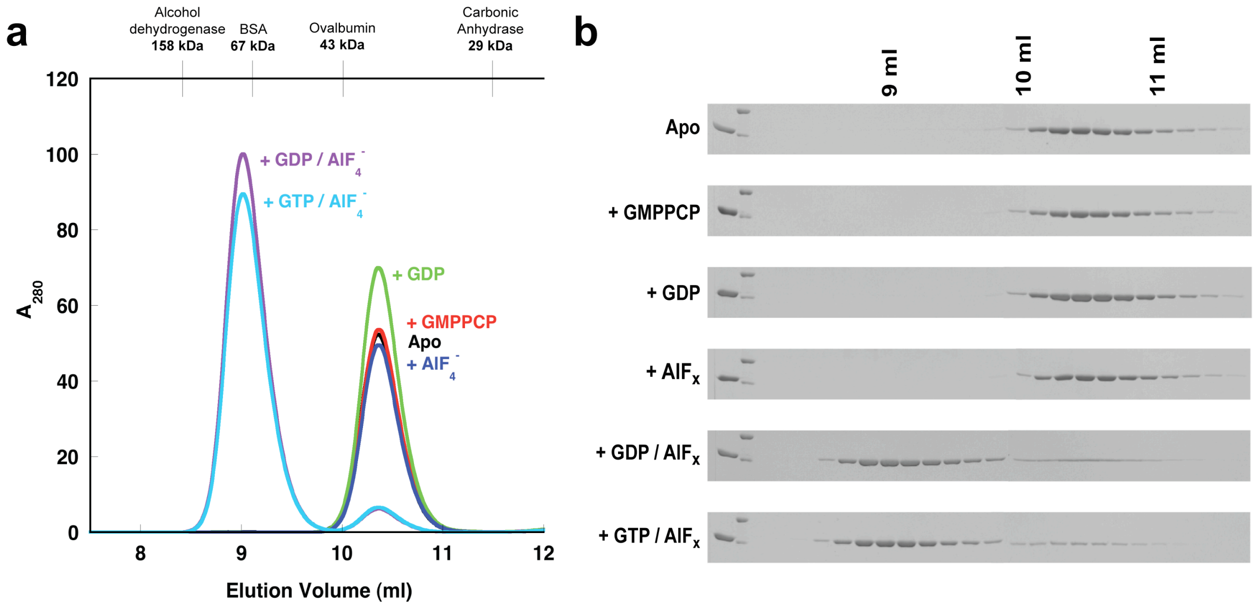

Supplementary Figure 2. Nucleotide-dependent dimerization of GG. a, Size exclusion chromatography (SEC) of GG in the presence of different guanine nucleotide analogs. GG (1 mg/ml) was incubated with each analog for 30 minutes at 37°C and then injected on to a Superdex 75 HR 10/30 column. Retention volumes for GG monomer and dimer are 10.37 ml and 9 ml respectively. Retention volumes for molecular weight standards are shown above. b, SDS-PAGE analysis of the SEC elution fractions corresponding to the peaks in A. Elution volume for the various fractions is indicated above. Left lanes contain purified GG monomer for reference followed by molecular weight standards (upper band is 50 kDa, lower band is 37 kDa).

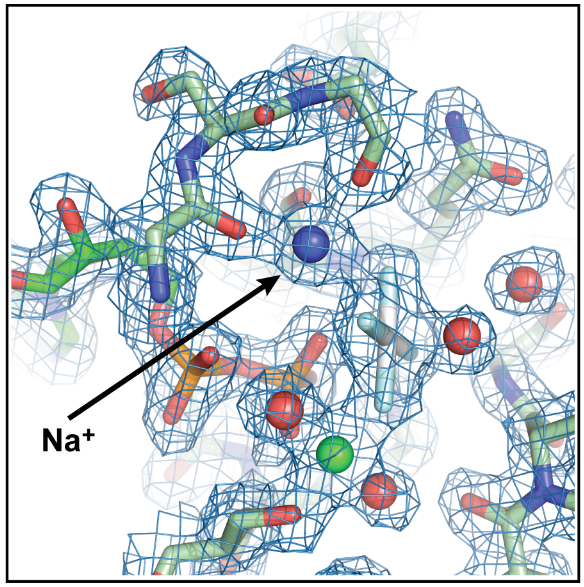

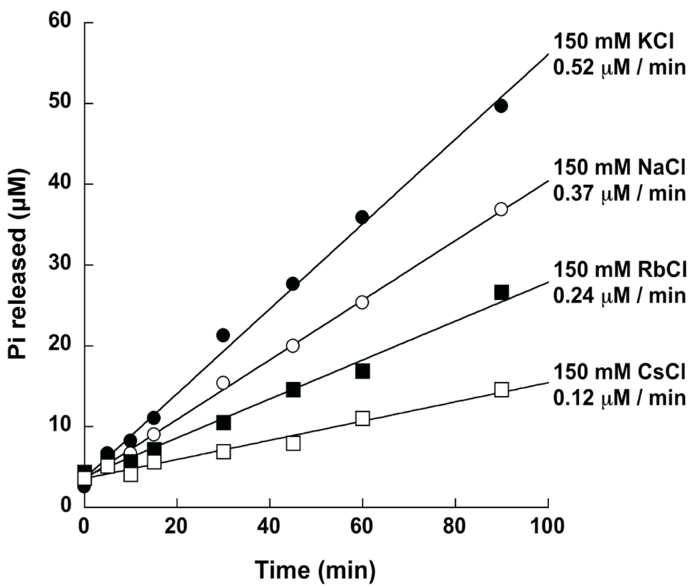

Supplementary Figure 3. Salt dependence of dynamin's GTPase activity. a, 2Fo-Fc map of GG active site. Black arrow denotes the additional electron density adjacent to aluminum fluoride that was modeled as a sodium ion (blue sphere). Red and green spheres indicate active site waters and bound magnesium ion respectively. Portions of switch I and switch II have been removed for clarity. b, Salt dependence of GG GTPase activity. GG activity was measured using 2 μM protein and 1 mM GTP after dialysis into buffers containing 20 mM Tris-HCl, pH 7.5, 1 mM $MgCl_2$, and 150 mM of either NaCl, KCl, RbCl, or CsCl. Representative time courses are shown.

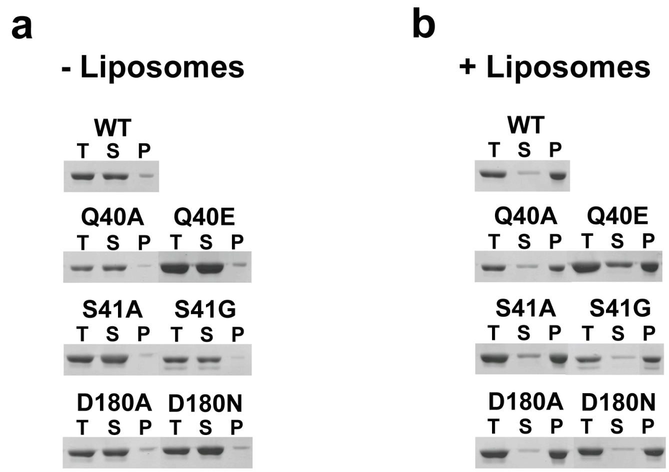

Supplementary Figure 4. Sedimentation profiles of Q40, S41, and D180 mutations in the presence and absence of liposomes. Sedimentation assay performed as described previously[17]. All mutants retain the capacity for membrane binding and self-assembly.

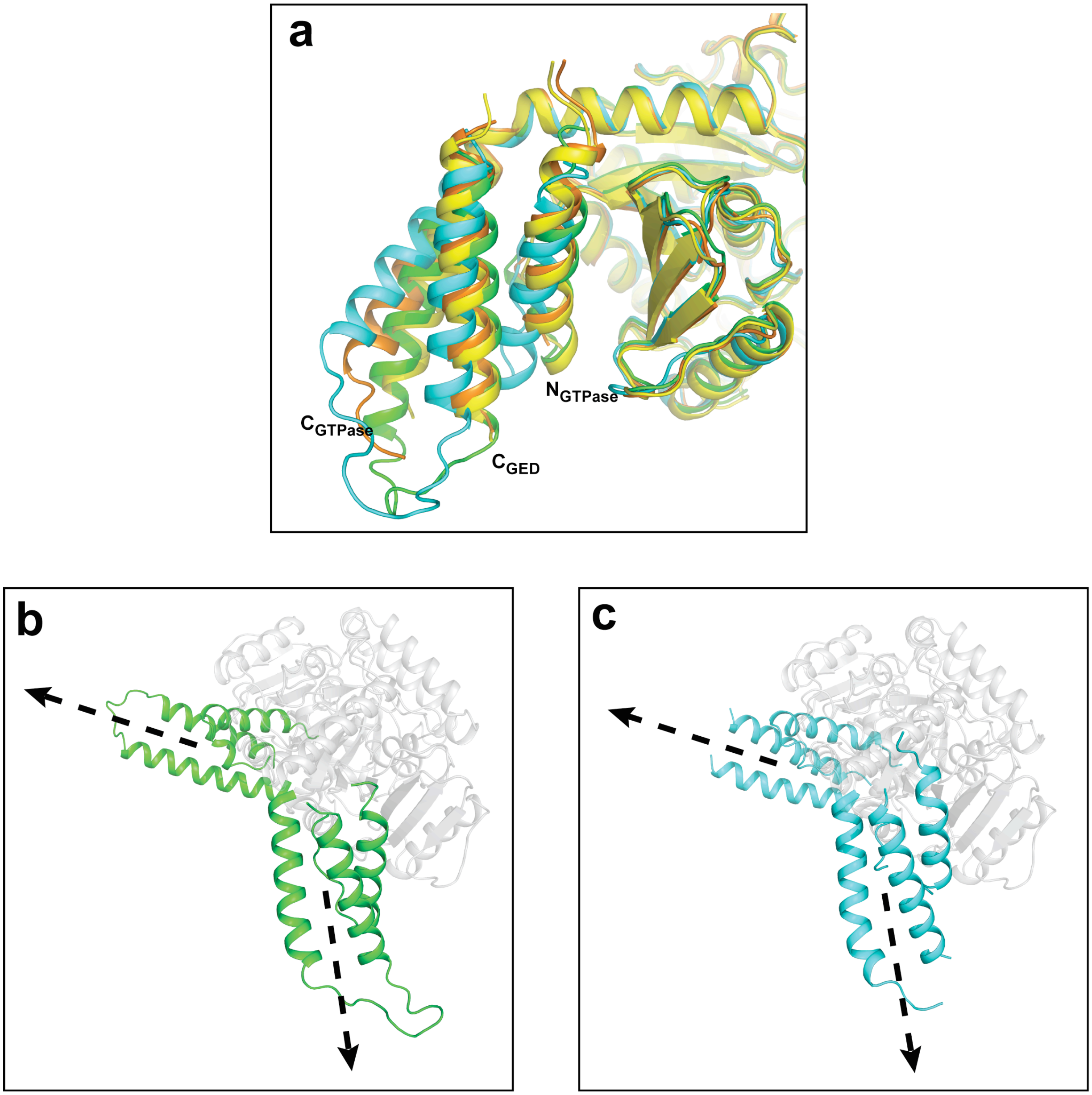

Supplementary Figure 5. Orientation of the BSEs within the GG dimer. a, Structural superposition of the individual GG monomers from both the long axis and short axis crystal forms. Coloring is as follows: long axis monomer A, green; long axis monomer B, cyan; short axis monomer A, yellow; short axis monomer B, orange. Each molecule was aligned to monomer A of the long axis structure. The N_{GTPase}, C_{GTPase} and C_{GED} helices are labeled. Note the variation in position of the BSEs relative the GTPase cores. b,c Relative configuration of the two BSEs within the long axis (b, green) and short axis (c, cyan) GG dimers. In each crystal form, the bundle from one monomer is oriented roughly perpendicular to its partner in the other monomer. The GTPase cores (gray) are rendered semi-transparent for clarity. Dashed arrows highlight the orientation of each bundle and denote the assumed position of the middle domain and GED that are connected to the C_{GTPase} and C_{GED} helices in full-length dynamin.

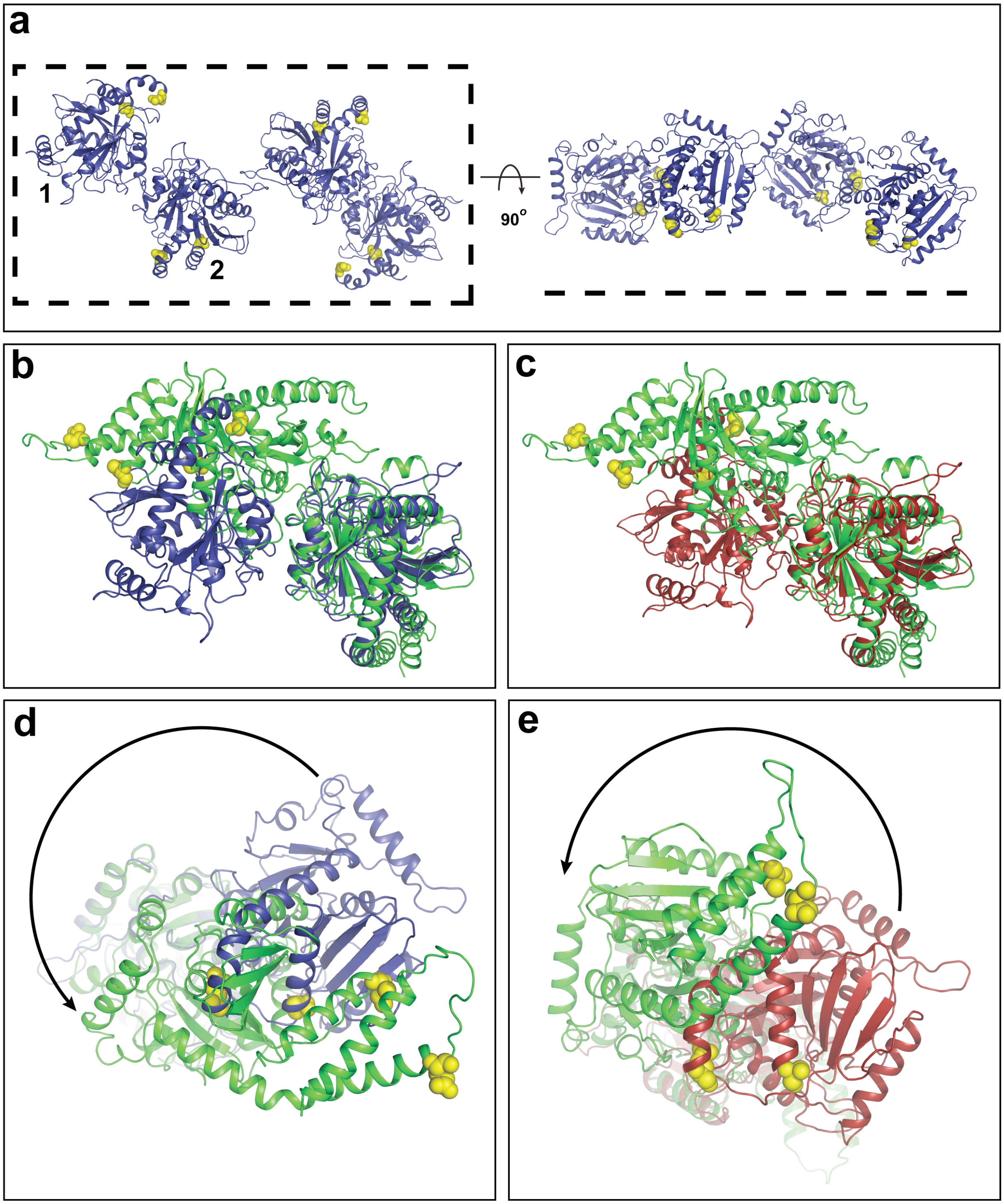

Supplementary Figure 6. Structural inconsistencies between the GG dimer and GTPase domain docking models. a, Structural model of the GTPase domain arrangement in the assembled dynamin polymer derived the computational docking of the nucleotide free rat dynamin G domain (blue) into the low-resolution cryo-EM density map of GMPPCP-bound ΔPRD dynamin in the constricted state[20]. Only two repeats of the asymmetric unit are shown as viewed from the top (left) and the side (right), with the individual G domain monomers labeled as 1 and 2. Dashed lines indicate the plane of the plasma membrane relative to these domains. Note that the GTPase domains in the model are oriented such that the C-termini of the N_{GTPase} and C_{GTPase} helices (yellow spheres) all face toward the membrane surface. b-e, Structural superposition of the GG dimer with the asymmetric unit GTPase docking model. Each monomer of the asymmetric unit was aligned to monomer A of the GG long axis structure (green) and the orientation of the additional docked monomer relative to GG monomer B was examined. The resulting alignments (blue for monomer 1, red for monomer 2) are viewed from the top in b and c respectively. The C-termini of GG's N_{GTPase} and C_{GTPase} helices are similarly marked with yellow spheres for comparison. Although the first docked monomer aligns well with GG monomer A in both cases, the second docked monomer is significantly displaced from GG monomer B. These differences are highlighted in d and e. In both alignments, a significant rotation (black arrow) would be required to reorient the second docked monomer into a position that is compatible with G domain dimerization.